

## Machine learning based prediction of COVID-19 mortality suggests repositioning of anticancer drug for treating severe cases

Thomas Linden, Frank Hanes, Daniel Domingo-Fernández, Lauren Nicole DeLong, Alpha Tom Kodamullil, Jochen Schneider, Maria J.G.T. Vehreschild, Julia Lanznaster, Maria Madeleine Ruethrich, Stefan Borgmann, Martin Hower, Kai Wille, Torsten Feldt, Siegbert Rieg, Bernd Hertenstein, Christoph Wyen, Christoph Römmele, Jörg Janne Vehreschild, Carolin E.M. Jakob, Melanie Stecher, Maria Kuzikov, Andrea Zaliani, Holger Fröhlich

### Angaben zur Veröffentlichung / Publication details:

Linden, Thomas, Frank Hanes, Daniel Domingo-Fernández, Lauren Nicole DeLong, Alpha Tom Kodamullil, Jochen Schneider, Maria J.G.T. Vehreschild, et al. 2021. "Machine learning based prediction of COVID-19 mortality suggests repositioning of anticancer drug for treating severe cases." *Artificial Intelligence in the Life Sciences* 1: 100020.  
<https://doi.org/10.1016/j.aailsci.2021.100020>.



## Research Article

## Machine Learning Based Prediction of COVID-19 Mortality Suggests Repositioning of Anticancer Drug for Treating Severe Cases



Thomas Linden<sup>a,b,#,\*</sup>, Frank Hanses<sup>c,q,#</sup>, Daniel Domingo-Fernández<sup>a</sup>, Lauren Nicole DeLong<sup>a,b</sup>, Alpha Tom Kodamullil<sup>a</sup>, Jochen Schneider<sup>d</sup>, Maria J.G.T. Vehreschild<sup>e</sup>, Julia Lanznaster<sup>f</sup>, Maria Madeleine Ruethrich<sup>g</sup>, Stefan Borgmann<sup>h</sup>, Martin Hower<sup>i</sup>, Kai Wille<sup>j</sup>, Torsten Feldt<sup>k</sup>, Siegbert Rieg<sup>l</sup>, Bernd Hertenstein<sup>l</sup>, Christoph Wyen<sup>m</sup>, Christoph Roemmele<sup>n</sup>, Jörg Janne Vehreschild<sup>e</sup>, Carolin E.M. Jakob<sup>o</sup>, Melanie Stecher<sup>p</sup>, Maria Kuzikov<sup>q</sup>, Andrea Zaliani<sup>q</sup>, Holger Fröhlich<sup>a,b,\*</sup>, on behalf of the LEOSS study group

<sup>a</sup> Fraunhofer Institute for Algorithms and Scientific Computing (SCAI), Schloss Birlinghoven, 53757 Sankt Augustin, Germany

<sup>b</sup> University of Bonn, Bonn-Aachen International Center for IT, Friedrich Hirzebruch-Allee 6, 53115 Bonn, Germany

<sup>c</sup> Emergency Department, University Hospital Regensburg, 93053 Regensburg, Germany

<sup>d</sup> Technical University of Munich, School of Medicine, University Hospital rechts der Isar, Department of Internal Medicine II, 81675 Munich, Germany

<sup>e</sup> Department II of Internal Medicine, Infectious Diseases, University Hospital Frankfurt, Goethe University, 60590 Frankfurt, Germany

<sup>f</sup> Department of Internal Medicine II, Hospital Passau, Innstraße 76, 94032 Passau, Germany

<sup>g</sup> Institute for Infection Medicine and Hospital Hygiene, University Hospital Jena, 07743 Jena, Germany

<sup>h</sup> Department of Infectious Diseases and Infection Control, Hospital Ingolstadt, 85049 Ingolstadt, Germany

<sup>i</sup> Department of Pneumology, Infectious Diseases and Intensive Care, Klinikum Dortmund gGmbH, Hospital of University Witten / Herdecke, 44137 Dortmund, Germany

<sup>j</sup> University Clinic for Haematology, Oncology, Haemostaseology and Palliative Care, Johannes Wesling Medical Centre Minden, 32429 Minden, Germany

<sup>k</sup> Department of Gastroenterology, Hepatology and Infectious Diseases, University Hospital Düsseldorf, Medical Faculty of Heinrich Heine University Düsseldorf, Moorenstrasse 5, 40225 Düsseldorf, Germany

<sup>l</sup> Department of Medicine II, University Hospital Freiburg, 79110 Freiburg, Germany

<sup>m</sup> Christoph Wyen, Praxis am Ebertplatz Cologne, 50668 Cologne, Germany

<sup>n</sup> Internal Medicine III - Gastroenterology and Infectious Diseases, University Hospital Augsburg, 86156 Augsburg, Germany

<sup>o</sup> Department I for Internal Medicine, University Hospital of Cologne, University of Cologne, 50931 Cologne, Germany

<sup>p</sup> Fraunhofer Institute for Translational Medicine and Pharmacologie (ITMP), Volkspark Labs, Schnackenburgallee 114, 22535 Hamburg, Germany

<sup>q</sup> Department for Infectious Diseases and Infection Control, University Hospital Regensburg, Germany

## ARTICLE INFO

## Keywords:

Machine learning  
Explainable ai  
Precision medicine  
Covid19  
Drug repositioning

## ABSTRACT

Despite available vaccinations COVID-19 case numbers around the world are still growing, and effective medications against severe cases are lacking. In this work, we developed a machine learning model which predicts mortality for COVID-19 patients using data from the multi-center 'Lean European Open Survey on SARS-CoV-2-infected patients' (LEOSS) observational study (>100 active sites in Europe, primarily in Germany), resulting into an AUC of almost 80%. We showed that molecular mechanisms related to dementia, one of the relevant predictors in our model, intersect with those associated to COVID-19. Most notably, among these molecules was tyrosine kinase 2 (TYK2), a protein that has been patented as drug target in Alzheimer's Disease but also genetically associated with severe COVID-19 outcomes. We experimentally verified that anti-cancer drugs Sorafenib and Regorafenib showed a clear anti-cytopathic effect in Caco2 and VERO-E6 cells and can thus be regarded as potential treatments against COVID-19. Altogether, our work demonstrates that interpretation of machine learning based risk models can point towards drug targets and new treatment options, which are strongly needed for COVID-19.

## 1. Introduction

As of October 2021, the ongoing SARS-CoV-2 pandemic led to almost 5 million reported deaths worldwide according to data

from the for US Institute for Health Metrics and Evaluation (<https://covid19.healthdata.org/>). In addition, economic costs are estimated to reach the order of several trillion dollars for the USA alone [11]. While effective vaccinations are now available, there are still a

\* Corresponding authors.

E-mail addresses: [thomas.linden@scai.fraunhofer.de](mailto:thomas.linden@scai.fraunhofer.de), [thomaz.linden@gmail.com](mailto:thomaz.linden@gmail.com) (T. Linden), [holger.froehlich@scai.fraunhofer.de](mailto:holger.froehlich@scai.fraunhofer.de) (H. Fröhlich).

# Authors contributed equally.

<https://doi.org/10.1016/j.ailsci.2021.100020>

Received 8 November 2021; Received in revised form 22 November 2021; Accepted 22 November 2021

Available online 17 December 2021

2667-3185/© 2021 The Authors. Published by Elsevier B.V. This is an open access article under the CC BY-NC-ND license

(<http://creativecommons.org/licenses/by-nc-nd/4.0/>)

considerable number of infected people worldwide. Moreover, effective medications for treating severe cases are still scarce. Remdesivir, a drug originally developed against the Ebola virus, is currently the only approved COVID-19 drug in the European Union, and evidence suggests that it has little effect on the overall survival of COVID-19 patients [5].

Several studies have revealed general risk factors for a poor disease outcome, such as age, male gender, and low platelet count [20,42,46,65]. In addition, machine learning (ML) models have been published to predict mortality risk for individual patients, primarily based on data from Intensive Care Units and electronic health records from the US and UK [3,6,19,31,48,53,57] as well as a few other countries [33,39]. Notably the 4C mortality score developed by Ali et al., based on data from the UK has recently been validated within an independent study in Canada [31]. None of these models have resulted in a change of clinical routine or the identification of new treatment options so far.

In this work, we specifically investigated data from nearly 5700 PCR or rapid test confirmed SARS-CoV-2 patients recruited in more than 100 European active sites, primarily all over Germany. For these patients, disease symptoms, vital parameters, biomarkers from urine and blood, and diagnosed comorbidities were available. Using these data and ML, we first developed a model that can predict mortality with an area under receiver operator characteristic curve (AUC) of almost 80% up to 60 days in advance. One of the relevant predictors in our model was a prior diagnosis of dementia, which increases the mortality risk by about 15%. Based on this finding, we explored the overlap between COVID-19, Alzheimer's (AD), and Parkinson's Disease (PD) molecular disease mechanisms, which pointed us to tyrosine kinase 2 (TYK2) as a potential new drug target. Finally, our experimental data with Caco2 and VERO-E6 cells suggests that Sorafenib and Regorafenib, two approved anti-cancer drugs, could be repositioned for treating severe COVID-19 cases.

## 2. Results

### 2.1. Overview about LEOSS data

The Lean European Open Survey on SARS-CoV-2 infected patients (LEOSS - <https://leoss.net/>) is an observational, multi-center study focusing on PCR or rapid test confirmed patients. Study centers are primarily University Medical Centers, but also include other hospitals, institutes, and medical practices. Active sites cover several European countries but have a primary focus on Germany. They are thought to generate representative data of (primarily hospitalized) COVID-19 cases, at least for Germany. In order to ensure anonymity in all steps of the analysis process, an individual LEOSS Scientific Use File (SUF) was created, which is based on the LEOSS Public Use File (PUF) principles described in [29]. The baseline data from more than 100 active sites, collected at time of a positive test or diagnosis, comprises patient demographics, disease symptoms, vital parameters, biomarkers from urine and blood, and comorbidities. Follow-up information, including survival, was available for patients between 18 and 85 years. These data were further filtered to only include patients with less than 50% of missing data at baseline, resulting into  $n = 5679$  patients (Table 1). Out of those 5679 patients, 5225 (92%) were inpatient, and 569 (10.0%) were reported death cases within a follow-up period of up to 78 days. Among them, 430 (76% of 569) patients were reported death cases within the first 20 days (Fig. 1).

### 2.2. Machine learning can predict mortality with high accuracy

We implemented and compared a broad panel of time-to-event machine learning models to predict patient survival using only LEOSS baseline data:

- Elastic net penalized Cox proportional hazards regression [10,66,71]
- Elastic net penalized Weibull accelerated failure time regression [35,62,71]

**Table 1**

Overview of patient demographics in LEOSS.

Age	
18 - 25 years	181
26 - 35 years	472
36 - 45 years	540
46 - 55 years	907
56 - 65 years	1125
66 - 75 years	981
76 - 85 years	1231
missing	242
Gender	
Male	3229
Female	2218
missing	232
Ethnicity	
Caucasian	4225
missing	1195
Asian & Pacific Islander	155
African & African American	98
Hispanic or Latino	6
Country	
Germany	5411
Turkey	65
Belgium	40
Czechia	33
Latvia	27
Other	26
GBR	23
Italy	19
Spain	15
France	11
Austria	9

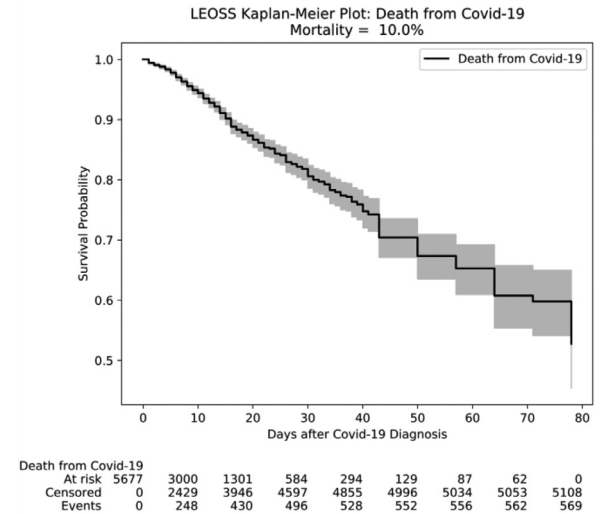


**Fig. 1.** Kaplan-Meier plot of COVID-19 patients in LEOSS. The plot shows the estimated survival function according to the well-known product limit estimator, see section “Methods” [32]. The gray area depicts the 95% confidence interval.

- DeepSurv – a neural network approach using a loss function derived from a Cox proportional hazard model [34]
- Random Survival Forests [28]
- XGBoost Survival Embeddings – a popular stochastic gradient boosting algorithm using a loss function derived from a Weibull regression [58]

Notably, all these models account for the right censoring of the data, see details in section “Methods”. We evaluated models via a five-fold cross-validation (CV). In other words, we split the entire dataset into five

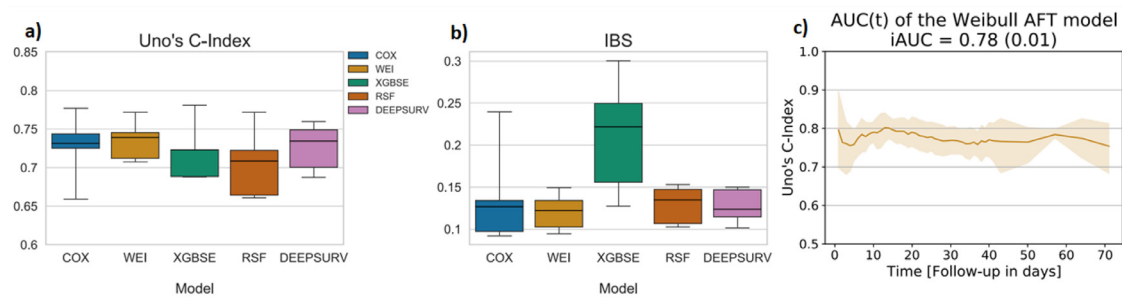


**Fig. 2.** (a) Model prediction performance measured via Uno's C-index on held out test sets (COX = elastic net penalized Cox proportional hazards regression; WEI = elastic net penalized Weibull accelerated failure time regression; XGBSE = XGBoost Survival Embeddings; RSF = Random Survival Forest; DEEPSURV = DeepSurv); (b) model calibration error measured via Integrated Brier Score (IBS) on held out test sets; (c) model prediction performance as function of time on held out test sets with 95% confidence interval, with integrated AUC (iAUC) denoting the mean (standard error) AUC over time. (For interpretation of the references to colour in this figure legend, the reader is referred to the web version of this article.)

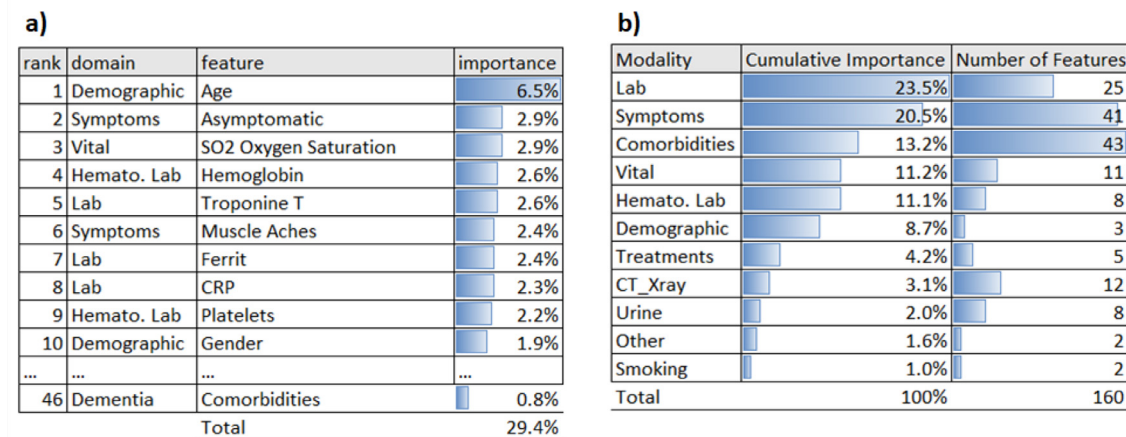


**Fig. 3.** Feature importance using absolute SHAP values: (a) top 10 predictors; (b) cumulative influence per feature modality. (For interpretation of the references to colour in this figure legend, the reader is referred to the web version of this article.)

outer folds, and we subsequently left out one of these folds for testing the model, while the rest of the data was used for model training and tuning. Notably, splitting of the data was performed in a stratified manner, such that the number of events was equally maintained across all folds. We tuned the hyper-parameters within the CV loop using an extra level of inner five-fold CV (see Section 4.2 for details). We employed Uno's C-index as a metric to assess prediction performance [56]. A C-index of 50% indicates chance level, whereas a C-index of 100% would reflect a perfect concordance of model predictions and observed death cases in the test data (see Section 4.3 for details).

Overall, elastic net penalized Weibull regression achieved the best discrimination performance with ~77% C-index (Fig. 2a) and low calibration error (Integrated Brier Score – IBS) of 0.12 (Fig. 2b, **Supplementary Table 1**). Furthermore, a stable prediction performance of ~80% AUC was found up to ~60 days after disease diagnosis (Fig. 2c). Therefore, elastic net penalized Weibull regression was used to subsequently train a final model on the entire dataset while using the previously described approach for hyper-parameter tuning.

### 2.3. Diagnosis of dementia as a relevant predictor

The final model was further explored with respect to the impact of most relevant predictors using Shapley Additive Explanations - SHAP [38]. Briefly, SHAP is an approach from cooperative game-theory to decompose the overall prediction of the model into a sum of individual feature contributions (see details in 4.4). In total, the final model comprised 160 features. A complete list can be found in **Supplementary File 1**.

Fig. 3a shows the most influential features according to SHAP, while Fig. 3b summarizes the influence of entire feature modalities, indicating that lab measures were the most relevant type of features (23.5% cumulative importance). Disease symptoms ranked second (20.5%) and comorbidities third (13.2% cumulative importance). Age, gender, platelet count as well as elevated troponin and ferritin concentrations were among the top predictors in the model, which are all known risk factors [20,42,46,65]. The prognostic significance of hemoglobin level and autoimmune hemolytic anemia for an unfavorable disease outcome has been discussed in [2]. The C-reactive protein (CRP) is a well-known infection and inflammation marker, which has been used as an indicator and prognostic marker of severity of COVID-19 infection [54]. Muscle pain is an often observed symptom of the infection [63], and its extent has been associated to the likelihood of a more unfavorable prognosis of hospitalized COVID-19 patients [12]. Comorbidity associated predictors included hypertension, an acute kidney injury, diabetes and dementia (**Supplementary Table 2, Supplementary File 2**). Again, this is concordant with the current literature [8,16,43].

Fig. 4 displays partial dependency plots for the previously discussed predictors, describing the quantitative relationship between individual feature attributes and their impact on estimated hazard ratios. Accordingly, an asymptomatic Covid-19 infection (Fig. 4b) resulted into an ~35% lower mortality risk compared to more severe disease symptoms, and for patients with low hemoglobin level (Fig. 4c) or low oxygen saturation (Fig. 4d) mortality risk was even increased by 50%. Prior diagnosis of dementia (Fig. 4d) results into an ~15% increased mortality risk after SARS-CoV-2-19 infection (hazard ratio dementia vs. non-dementia: ~1.15; 95% CI: [1.08, 1.24]). Notably, there are different possible ex-

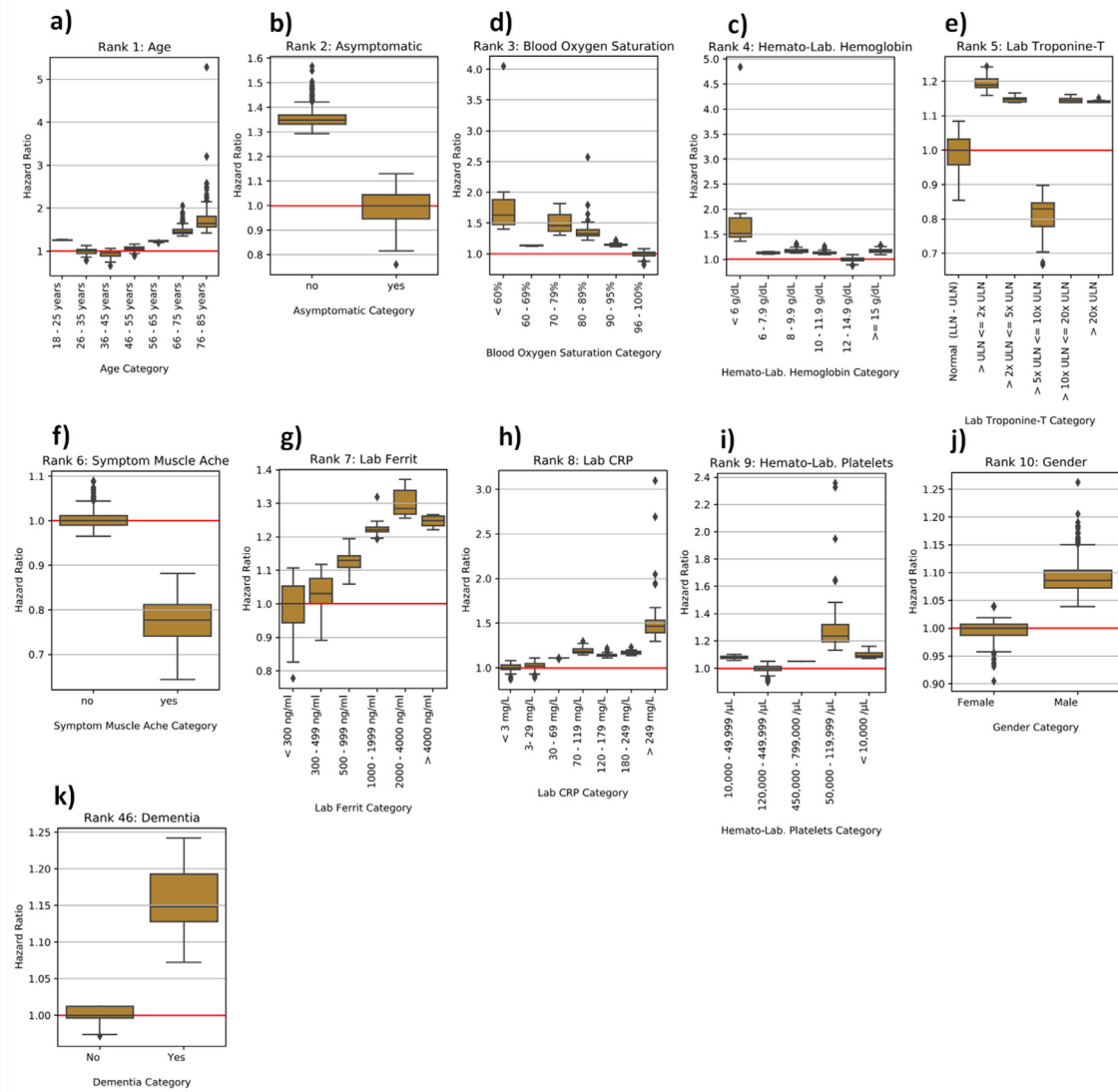


**Fig. 4.** Partial dependence plots for most influential predictors. Boxplots show the distribution of patient specific hazard ratios per variable category. The red horizontal line defines the reference. The hazard ratio describes by which factor the median lifetime is expected to change compared to reference. (For interpretation of the references to colour in this figure legend, the reader is referred to the web version of this article.)

planations for this finding: (a) dementia might be a proxy for age; (b) dementia might, independently of age, trigger biological, physiological and psychological mechanisms that contribute to an unfavorable disease outcome.

#### 2.4. Commonly affected molecular mechanisms between neurodegenerative disorders and COVID-19

We aimed for a more in-depth exploration of potential overlaps of neurodegeneration and COVID-19 disease mechanisms. Notably, there has been increasing evidence that SARS-CoV-2 can enter the central nervous system [7,36,41], raising the question of potential interactions with dementia disease pathologies. In this context, [70] recently reported an overlap of transcriptionally dysregulated biological pathways in a very limited number of patients with Alzheimer's Disease (AD) and COVID-19.

Here, we focused more broadly on shared molecular mechanisms linking COVID-19 with AD as well as Parkinson's Disease (PD), another major neurodegenerative disorder, which has previously been associated with an increased risk for an unfavorable outcome of a SARS-CoV-

2 infection [50,59]. By looking at the intersection between AD and PD cause-and-effect models (referred as knowledge graphs - KGs) and the corresponding COVID-19 KG, in this work we found a series of mechanisms that were shared between all three disease etiologies (**Supplementary Table 3**).

Firstly, one of the mechanisms identified by our approach is related to three proteins involved in the innate immune system (i.e., DDX58, MAVS, and IFIH1), and more specifically in the detection and response to viruses. These proteins are involved in both indications. For example, MAVS interacts with the RNA helicase RIG-I/MDA-5 after the dsRNA of the virus is recognized, leading to the initiation of the antiviral signaling cascade [69]. Related with this process is the second shared mechanism, which corresponds to the activation of the inflammasome and the subsequent triggering of caspase activation through cytokine secretion. This mechanism has been strongly linked with both AD [21] and PD [61] as well as COVID-19 [44]. In the context of neurodegeneration, the activation of the inflammasome leads to the secretion of inflammatory cytokines and cell death through pyroptosis, to which both AD and PD are associated via tangle and plaque formation and death of dopamine neurons, respectively [4]. Similarly, in the context of COVID-19, the in-



flammasome is activated by the proteins of the SARS-CoV-2 virus, which in turn leads to the production of inflammatory molecules, and in some cases leads to hyperinflammation [44]. Finally, TYK2 is also present in all three KGs. It is known to be implicated in the regulation of apoptosis in the amyloid cascade of AD [60] as well  $\alpha$ -synuclein-induced neuroinflammation and dopaminergic neurodegeneration [47].

Lastly, IL-6 and IL-10 are among two of the interleukins secreted after inflammasome activation, one of the shared mechanisms between these pathologies, and their increased expression has been shown to be predictive of COVID-19 severity [14]. Furthermore, the interaction between two other proteins (i.e., DDIT3 and BCL2L11) involved in the regulation of apoptosis is also suggested as a common mechanism across these indications [18,26].

## 2.5. Sorafenib and regorafenib as potential treatments against COVID-19

In the following, we specifically focused on TYK2, which is a protein involved into the amyloid cascade. TYK2 inhibition results into effective regulation of IFN $\alpha$ , IL-10, IL-12, and IL-23 [23], which has specifically been reported in neurodegenerative disorders [45]. TYK2 has been patented as drug target in AD (CN102112879B, China, [27]). In addition, genetic variants in TYK2 have recently been associated to COVID-19 disease severity [9]. Moreover, we found several kinase inhibitors active against SARS-CoV-2 in a cellular screen for anti-cytopathic effect (anti-CPE) in two different cellular environments: Caco2 [17] and VERO-E6 [67]. The relative results of those screening have been made public on ChEMBL ([https://www.ebi.ac.uk/chembl/document\\_report\\_card/CHEMBL4303101/](https://www.ebi.ac.uk/chembl/document_report_card/CHEMBL4303101/), [https://www.ebi.ac.uk/chembl/document\\_report\\_card/CHEMBL4495565/](https://www.ebi.ac.uk/chembl/document_report_card/CHEMBL4495565/)), respectively.

We challenged VERO-E6 cells with SARS-CoV-2 pretreated with compounds from the Fraunhofer Repurposing Library (5632 compounds - [https://www.itmp.fraunhofer.de/en/innovation-areas/drug\\_screening](https://www.itmp.fraunhofer.de/en/innovation-areas/drug_screening)

[repurposing.html](https://ecbd.eu/compound/#lib{value='2'}lib{value='2'})), the EUOS Bioactives library (~2500 compounds - <https://ecbd.eu/compound/#lib{value='2'}lib{value='2'}>), and a proprietary “Safe in Man” library of compounds having passed phase I clinical trial (~600 compounds). Regarding the phenotypic assay with Caco2 cells to determine compound antiviral activity, we adapted a previously published protocol [37]. Compounds were added to confluent layers of Caco-2 cells in MEM supplemented with 1% FBS in 96-well plates. For the primary screen final compound concentration was 10  $\mu$ M (0.1% DMSO final) in singlicates. Dose response profiling of selected priority compounds was performed with a range of eight different concentrations in three independent replicates (maximum 20  $\mu$ M, minimum 20 nM, half log dilution factor, 0.1% DMSO final). Following the addition of compounds, cells were immediately infected with SARS-CoV-2 at MOI 0.01. Control wells (+ virus and - virus) also contained DMSO at 0.1% DMSO final. After 48 h, cells were fixed using 3% PFA in PBS, and the plates sealed and disinfected to inactivate SARS-CoV-2. Quantification of viral inhibition (based upon Caco-2 cell viability relative to controls) was performed using high content imaging (PerkinElmer, Operetta CLS). For what concerns the assay on VERO-E6 cells, we used basically the same protocol, but the time we waited for readout was longer than 48 h (96 h) due to the different infection kinetic on these cells.

In VERO-E6 cells, only Regorafenib showed a clear antiviral CPE potency with an IC<sub>50</sub> of around 3–5  $\mu$ M. In Caco2 cells, Sorafenib and Regorafenib demonstrated a similar antiviral CPE potency with an IC<sub>50</sub> of around 1  $\mu$ M for both molecules (Fig. 5). Both compounds are reported to be non-selective JAK/TYK2 inhibitors [25]. While the involvement of the JAK kinase family in inflammatory cytokine modulation is well-known, the extent of which TYK2 (a JAK family member) could be responsible of the observed CPE effect remains to be determined with more selective drug candidates. Such TYK2 selective preclinical compounds are currently not part of our screened libraries, because we focused on repurposing marketed kinase inhibitors.

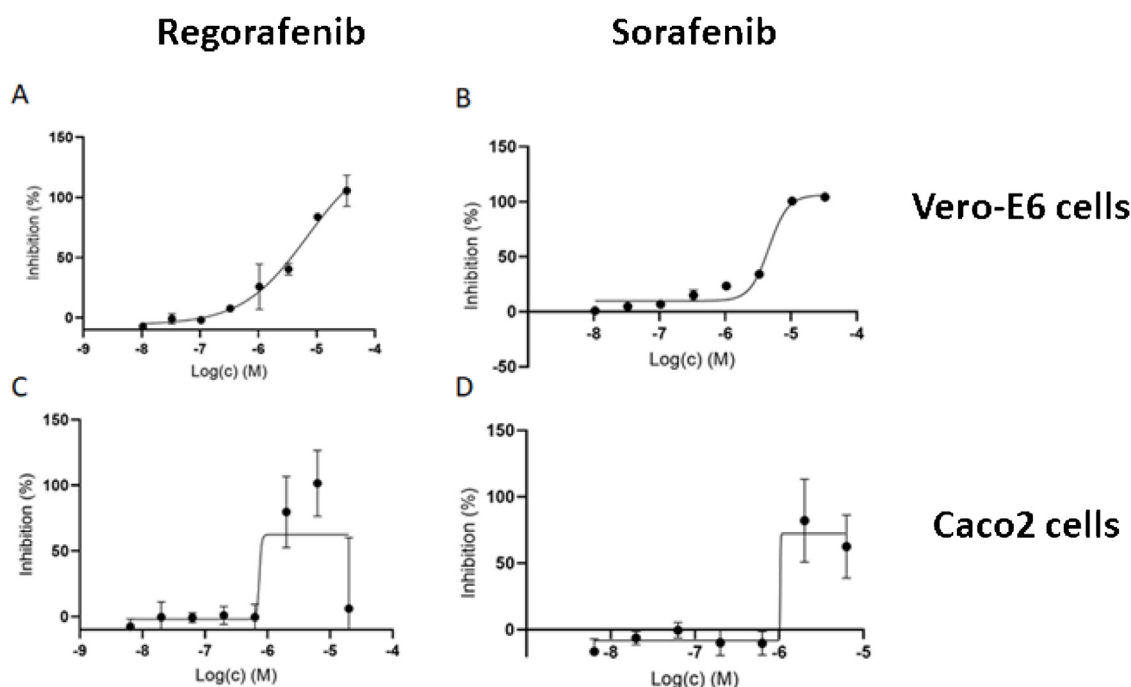


**Fig. 5.** Regorafenib (panels A and C) and Sorafenib (panels B and D) activities measured in different cell lines (Vero-E6 cells upper panels; Caco2 cells lower panels) as percentage inhibition of viral cytopathic effect normalized to Remdesivir as positive control (100%). Cells in wells were treated with SARS CoV-2 virus, and drugs were administered after 48 or 96 h after infection. Subsequently, cells were stained, washed and counted if alive. Some signs of toxicity on Caco2 cells (lower panels) started to surface at higher drug concentrations and this might be the reason for the higher observed variance of triplicates. The slightly negative relative inhibition shown in panel D is caused by plate control differences within plates.

### 3. Conclusion

As of October 2021, the rates of completely vaccinated individuals in many Western countries are stagnating between 60 – 70%, while the fraction of vaccinated individuals is globally only around 36% [40]. Correspondingly, case numbers in many countries around the world are still increasing. Hence, there is an unmet need for effective and cost-efficient medications against severe cases.

In this work, we first developed a highly predictive ML model for predicting COVID-19 mortality on an individual patient basis using deep observational data from LEOSS, primarily covering the inpatient situation in Germany (95% of patients). To our knowledge, this is the first ML based mortality model based on such (notionally) representative German data. Notably, ML models predicting alternative endpoints using LEOSS have been published recently [30,64].

Our ML model demonstrates similar prediction performance to the well-known 4C mortality score, which has been developed based on representative data from the UK [3]. However, a direct comparison between both models is not possible, because the 4C model is formulated as a classifier predicting all-cause in-hospital mortality, whereas our model is formulated as a time-to-event model predicting all-cause time dependent mortality risk after COVID-19 diagnosis. Our model, thus, considers censoring of survival times after patients have left hospital or other medical facilities. Our mortality model was built on a set of patients, which is thought to be primarily representative for German hospitals. Whether there are unknown selection biases, remains an open question and they were not under our control. Moreover, it is unclear whether our model would be predictive for patients in other countries.

We showed that dementia, as one of the relevant predictors in our model, intersects on a molecular mechanism level with COVID-19. Together with evidence from recent GWAS studies, this pointed us to TYK2 as a potential drug target for COVID-19. Using a cellular screening assay for anti-cytopathic effect, we identified the anti-cancer drugs Regorafenib and Sorafenib as potential drug candidates against COVID-19. Notably, the known association of JAK family inhibitors like Regorafenib and Sorafenib with cellular inflammatory cytokines can be further characterized by investigating transcription dynamics within the first 12 h after SARS-CoV-2 viral infection compared to mock control [55]. Based on such data, Stukalov et al. [55], tested both compounds in the A549-ACE2 cell line and reported increased virus growth after treatment. Other authors recently reported Sorafenib to be a potent STING inhibitor effectively stopping virus growth in THP1 cells and thus suggested to pay more attention to COVID-19 treatment strategies that address the dysregulation of cytokines [13]. Since the used cell lines in both cases were different from ours, results are not directly comparable. Hence, we see a need for further tests with Regorafenib and Sorafenib in other cell systems.

In addition to further experimental validation of Regorafenib and Sorafenib, it could be interesting to explore in large scale clinical real-world data whether SARS-CoV-2 infected patients treated with Regorafenib or Sorafenib demonstrate a lower mortality than other SARS-CoV-2 patients.

Overall, our work demonstrates that interpretation of an ML based risk model trained on rich data can point towards drug targets and new treatment options, which are strongly needed for COVID-19.

### 4. Methods

#### 4.1. Kaplan-Meier estimator

The Kaplan-Meier product limit estimator is classical non-parametric statistic to estimate a survival function  $S(t)$  [32]: Let  $t_i$  denote a time point, where at least one event / death happened. The number of events (deaths) at  $t_i$  is denoted as  $d_i$ , and the number of individuals known to have survived up to  $t_i$  is  $n_i$ . Then the Kaplan-Meier estimator  $\hat{S}(t)$  of the survival function (representing the probability that life is longer than  $t$ )

is given by:

$$\hat{S}(t) = \prod_{i: t_i \leq t} \left(1 - \frac{d_i}{n_i}\right)$$

and  $\hat{S}(0) = 1$ .  $\hat{S}(t)$  is a right-continuous step function with jumps at event times  $t_i$ . Censoring at certain time points affect the estimate only by reducing the number of individuals that are at risk for a subsequent event.

#### 4.2. Machine learning models for predicting COVID-19 mortality

We compared five different machine learning algorithms, as outlined in Section 2.2. Here, we only elaborate on the best performing one, namely the elastic net penalized Weibull regression: The elastic net is a regularization and variable selection method, to shrink coefficients using a linear combination of  $L_1$  and  $L_2$  penalties. The Weibull regression is an accelerated failure time (AFT) model, which means that covariates act multiplicatively on (survival) time. It is used if the proportional hazards assumption of the Cox model is not satisfied. AFT models allow to directly estimate (the effect of covariates on) expected failure times, where the time until failure is the duration of survival.

Let  $i \in \{1, \dots, n\}$  denote the  $i$ -th patient with covariate vector  $x_i \in \mathbb{R}^p$  and observed follow-up time  $T_i$ . Furthermore, let  $\delta_i \in \{0, 1\}$  be an event indicator (0 = right censored, 1 = uncensored) at  $T_i$ . The true and potentially unobserved survival time is  $Z_i$ , and the censoring time is  $C_i$ . That means  $T_i = \min(Z_i, C_i)$  and  $\delta_i = 1\{T_i = Z_i\}$ . The censoring is supposed to be non-informative about the true survival time [49]. In a Weibull AFT model, we assume  $Z_i|x_i \sim \text{Weibull}(\gamma, \zeta)$ , i.e. the hazard function has the form

$$h(Z_i|x_i) = \exp(\beta^T x_i) \zeta \gamma Z_i^{\gamma-1}$$

Parameters of a standard Weibull AFT model can be estimated by maximizing the likelihood [68]:

$$L(\beta, \gamma, \zeta) = \prod_{i=1}^n h(T_i|x_i)^{\delta_i} S(T_i|x_i)$$

where  $S(\cdot)$  denotes the survival function  $S(T_i|x_i) = \exp\{-\int_0^{T_i} h(s|x_i)ds\}$ .

To account for overfitting, our case coefficients  $\beta$  were additionally penalized via the elastic net penalty:

$$\Omega(\beta) = \alpha \lambda \|\beta\|_1 + (1 - \alpha) \lambda \|\beta\|_2^2$$

Hyperparameters (i.e.  $\alpha, \lambda$ ) were tuned with Bayesian hyperparameter optimization using the Optuna package [11] within the inner-loop of the nested cross-validation. Early stopping was used if applicable (DeepSurv, GBM, XGBSE), and the best candidate model was subsequently selected. We chose the 5-fold cross-validated Harrell's C-index [22] as objective for the hyperparameter tuning. We ran the optimization for twenty initial epochs, adopted the search space if reasonable, and then ran it for another twenty rounds. Thus, forty hyperparameter sets were evaluated and the resulting best combination was selected based on the highest objective function value. Using this hyperparameter set, we subsequently trained a model on the entire training data and evaluated it on the held-out test set.

#### 4.3. Uno's concordance-index

The prediction performance of time-to-event models can be evaluated with respect to discriminating between subjects with different event times via Uno's C-index [56]: The C-index (Concordance index) is a generalization of the area under receiver operator characteristic curve (AUC) for time-to-event models [24,51]. A value of 100% means perfect discriminative performance, and 50% is comparable to random predictions.

In essence, Uno's C is a rank correlation between the risk predictions and the observed event times. The C-index measures the concordance

across all pairs of patients  $(i, j)$ ,  $i \neq j$ . A pair is classified concordant if the predicted risk is higher for the patient with lower survival time. Uno's C-index was developed as an alternative to Harrell's C-index in settings with high censoring rates and leads to consistent concordance estimates under the general random censoring assumption. Uno's C-index uses an inverse probability censoring weighting (IPCW) approach [56]:

$$\hat{C}_{Uno} = \frac{\sum_{i \neq j}^n \delta_i \hat{G}(t_i)^{-2} I(t_i < t_j | t_i < \tau) I(\hat{h}_i > \hat{h}_j)}{\sum_{i \neq j}^n \delta_i \hat{G}(t_i)^{-2} I(t_i < t_j | t_i < \tau)}$$

The numerator counts the concordant pairs and the denominator the valid pairs, respectively. For patients  $i \in \{1, \dots, n\}$ ,  $\delta_i$  is 1 if an event (death) was observed and otherwise 0,  $\hat{G}(\cdot)$  is the Kaplan-Meier estimator for the *censoring distribution* for IPCW,  $\hat{h}_i$  is the risk prediction of the  $i$ -th patient,  $t_i$  is the observed time and  $\tau$  is a stability parameter, for further details see [56].

#### 4.4. Feature importance using SHAP

Shapley Additive Explanations [38] are a model-agnostic approach from coalitional game theory. The assumption of this framework is, that individuals (feature attributes) are cooperating as a team (patient feature vector) for a joint outcome (model prediction). SHAP's goal is to estimate those individual contributions to the outcome. Key properties are a) the solution is unique; b) local exactness, which means the sum of feature contributions matches the output; c) if a feature has no impact, then it's SHAP-value is zero.

Mathematically, additivity and property b) can be described as:

$$f(x) = g(x') = \phi_0 + \sum_{i=1}^M \phi_i x'_i$$

$$x = h_x(x')$$

with  $f(x)$  being the original model and  $g(x')$  the explanation model defined on simplified inputs  $x' \in \{0, 1\}^M$ . Moreover,  $h_x(\cdot)$  is a function mapping  $x$  to the simplified input  $x'$ .  $\phi_i \in \mathbb{R}$  is the SHAP value of the  $i$ -th feature for the model input vector  $x$  and  $\phi_0$  denotes the expectation value of  $f(x)$ . In other words: The SHAP values  $\phi_i$  quantifies how much a particular feature pushes the prediction away from the population average  $\phi_0$ . SHAP values  $\phi_i$  are computed as follows:

$$\phi_i(f, x) = \sum_{S \subseteq F \setminus \{i\}} \binom{|F|}{|S|}^{-1} [f_{S \cup \{i\}}(x_{S \cup \{i\}}) - f_S(x_S)]$$

In other words, SHAP values are defined as a weighted (binomial coefficient) sum of the differences between (in square brackets) "prediction including the feature" minus "prediction excluding the feature", for any subset  $S$  in the power set  $F$ .  $f_{S \cup \{i\}}$  denotes the model trained with feature  $i$  included and  $f_S$  without it. Similarly,  $x_{S \cup \{i\}}$  denotes the feature subset with feature  $i$  included and  $x_S$  without it.

#### 4.5. Confidence intervals for hazard ratios

To construct a confidence interval for the hazard ratio of "dementia vs. non-dementia" we performed a bootstrap: We resampled 100,000 times with replacement a pair of a demented and non-demented patient. We then calculated the ratio of the SHAP values for the feature "prior dementia diagnosis" for both patients.

#### 4.6. Identification of common molecular mechanisms between COVID-19 and neurodegenerative diseases

To identify the shared molecular mechanisms between COVID-19, AD, and PD, we leveraged several resources listed in **Supplementary Table 3**. These were combined into two independent Knowledge Graphs (KGs) following the harmonization procedure described in our previous

work [52] and [15]. By doing so, we combined disease specific molecular interactions pertaining to COVID-19 and two neurological indications (i.e., AD and PD) into graph structures: one for COVID-19 and one for AD and PD. Subsequently, we calculated the intersection of these graphs. **Supplementary File 2** contains the corresponding shared mechanisms as an Excel table.

#### Author contributions

Drafted the manuscript: HF, TL, DDF, AZ; initiated and guided the project: HF; implemented machine learning models: TL; computational drug target identification: DDF, LDL, ATK; experimental validation: MK, AZ. Other authors: acquisition and preparation of LEOSS data

#### Funding

This work has been funded via the 'COPERIMOpus' initiative and supported by the Fraunhofer 'Internal Programs' under Grant No. Anti-Corona 840266.

The LEOSS registry was supported by the German centre for Infection Research (DZIF) and the Willy Robert Pitzer Foundation.

#### Ethics approval

LEOSS is registered at the German Clinical Trials Register (DRSK, S00021145) and was approved by the leading Ethics Committee No. 20–600 "Ethikkommission des Fachbereichs Humanmedizin der Johann-Wolfgang-Goethe-Universität Frankfurt am Main, 60590 Frankfurt, Germany". For the anonymization procedure see [29].

#### Code availability

The source code of the analyses presented in this paper is available at <https://github.com/thomasmoon/leoss-cov19>.

#### Declaration of interests

The authors declare that they have no known competing financial interests or personal relationships that could have appeared to influence the work reported in this paper.

#### Acknowledgments

We express our deep gratitude to all study teams supporting the LEOSS study. The LEOSS study group contributed at least 5 per mille to the analyses of this study: University Hospital Regensburg (Frank Hanses), Technical University of Munich (Christoph Spinner), University Hospital Frankfurt (Maria Vehreschild), Hospital Passau (Julia Lanznaster), University Hospital Jena (Maria Madeleine Ruethrich), Hospital Ingolstadt (Stefan Borgmann), Klinikum Dortmund gGmbH (Martin Hower), Johannes Wesling Hospital Minden Ruhr University Bochum (Kai Wille), University Hospital Duesseldorf (Bjoern-Erik Jensen), University Hospital Freiburg (Siegbert Rieg), Hospital Bremen-Center (Bernd Hertenstein), Practice at Ebertplatz Cologne (Christoph Wyen), University Hospital Augsburg (Christoph Roemmele), University Hospital Schleswig-Holstein Luebeck (Jan Rupp), Robert-Bosch Hospital Stuttgart (Katja Rothfuss), Catholic Hospital Bochum (St. Josef Hospital) Ruhr University Bochum (Kerstin Hellwig), Elisabeth Hospital Essen (Ingo Voigt), Hospital Maria Hilf GmbH Moenchengladbach (Juergen vom Dahl), Marien Hospital Herne Ruhr University Bochum (Timm Westhoff), Municipal Hospital Karlsruhe (Christian Degenhardt), University Hospital Heidelberg (Uta Merle), University Hospital Munich/ LMU (Michael von Bergwelt-Baildon), Hospital Leverkusen (Lukas Eberwein), University Hospital Wuerzburg (Nora Isberner), University Hospital Essen (Sebastian Dolff), Hospital St. Joseph-Stift Dresden



(Lorenz Walter), Hospital Ernst von Bergmann (Lukas Tometten), University Hospital Erlangen (Richard Strauss), University Hospital Cologne (Norma Jung), University Hospital Tuebingen (Siri Göpel), Bundeswehr Hospital Koblenz (Dominic Rauschnig), Hacettepe University (Murat Akova), University Hospital of Giessen and Marburg (Janina Trauth), Hospital Fulda (Philipp Markart), National MS Center Melsbroek (Marie D'Hooghe), Evangelisches Hospital Saarbrücken (Mark Neufang), Malteser Hospital St. Franziskus Flensburg (Milena Milovanovic), University Hospital Schleswig-Holstein Kiel (Anette Friedrichs), University Hospital Ulm (Beate Gruener), Center for Infectiology Prenzlauer Berg Berlin (Stephan Grunwald), Elbland Hospital Riesa (Joerg Schubert), University Hospital Saarland (Robert Bals), Clinic Munich (Wolfgang Gugge-mos), Agaplesion Diakonie Hospital Rotenburg (David Heigener), Hospital Braunschweig (Jan Kielstein).

The LEOSS study infrastructure group: Jörg Janne Vehreschild (Goethe University Frankfurt), Susana M. Nunes de Miranda (University Hospital of Cologne), Carolin E. M. Jakob (University Hospital of Cologne), Melanie Stecher (University Hospital of Cologne), Lisa Pilgram (Goethe University Frankfurt), Nick Schulze (University Hospital of Cologne), Sandra Fuhrmann (University Hospital of Cologne), Max Schons (University Hospital of Cologne), Annika Claßen (University Hospital of Cologne), Bernd Franke (University Hospital of Cologne) und Fabian Praßer (Charité, Universitätsmedizin Berlin).

## Supplementary materials

Supplementary material associated with this article can be found, in the online version, at doi:10.1016/j.aillsci.2021.100020.

## References

- Akiba Takuya, et al. Optuna: a Next-Generation Hyperparameter Optimization Framework. In: *Proceedings of the 25th ACM SIGKDD International Conference on Knowledge Discovery & Data Mining, KDD '19*. New York, NY, USA: Association for Computing Machinery; 2019. p. 2623–31. September 30, 2021. doi:10.1145/3292500.3330701.
- Algassim Abdulrahman A, et al. Prognostic Significance of Hemoglobin Level and Autoimmune Hemolytic Anemia in SARS-CoV-2 Infection. *Ann. Hematol.* 2020. <https://www.meta.org/papers/prognostic-significance-of-hemoglobin-level-and/> 32918594 November 21, 2021.
- Ali Rashid, et al. Isaric 4c Mortality Score As A Predictor Of In-Hospital Mortality In Covid-19 Patients Admitted In Ayub Teaching Hospital During First Wave Of The Pandemic. *Journal of Ayub Medical College, Abbottabad: JAMC* 2021;33(1):20–5.
- Anderson Faith L, et al. Plasma-Borne Indicators of Inflammation Activity in Parkinson's Disease Patients. *NPJ Parkinson's disease* 2021;7(1):2.
- Ansems Kelly, et al. Remdesivir for the Treatment of COVID-19. *Cochrane Database of Systematic Reviews* 2021(8). <https://www.cochranelibrary.com/cdsr/doi/10.1002/14651858.CD014962/full> October 18, 2021.
- Banoei Mohammad M, Dinparastisaleh Roshan, Zadeh Ali Vaeli, Mirsaedi Mehdi. Machine-Learning-Based COVID-19 Mortality Prediction Model and Identification of Patients at Low and High Risk of Dying. *Critical Care* 2021;25(1):328 October 18, 2021. doi:10.1186/s13054-021-03749-5.
- Boldrini Maura, Canoll Peter D, Klein Robyn S. 'How COVID-19 Affects the Brain. *JAMA Psychiatry* 2021;78(6):682–3 October 18, 2021. doi:10.1001/jamapsychiatry.2021.0500.
- Corona Giovanni, et al. Diabetes Is Most Important Cause for Mortality in COVID-19 Hospitalized Patients: systematic Review and Meta-Analysis'. *Rev Endocr Metab Disord* 2021;22(2):275–96.
- COVID-19 Host Genetics Initiative Mapping the Human Genetic Architecture of COVID-19'. *Nature* 2021;1–8.
- Cox DR. Regression Models and Life-Tables. *Journal of the Royal Statistical Society. Series B (Methodological)* 1972;34(2):187–220.
- Cutler David M, Summers Lawrence H. 'The COVID-19 Pandemic and the \$16 Trillion Virus. *JAMA* 2020;324(15):1495–6 October 18, 2021. doi:10.1001/jama.2020.19759.
- Demirel Esra, et al. A Relationship between Musculoskeletal Pain and Prognosis in Hospitalized COVID-19 Patients. *Journal of Health Sciences and Medicine* 2021;4(3):300–5. <https://dergipark.org.tr/en/pub/jhsm/899515> November 21, 2021.
- Deng, Xiaobing, Xiaoyu Yu, and Jianfeng Pei. 2020. 'Regulation of Interferon Production as a Potential Strategy for COVID-19 Treatment'. *arXiv:2003.00751 [q-bio]*. <http://arxiv.org/abs/2003.00751> (October 21, 2021).
- Dhar Sujan K, et al. IL-6 and IL-10 as Predictors of Disease Severity in COVID-19 Patients: results from Meta-Analysis and Regression. *Heliyon* 2021;7(2):e06155.
- Domingo-Fernández Daniel, et al. Multimodal Mechanistic Signatures for Neurodegenerative Diseases (NeuroMMSig): a Web Server for Mechanism Enrichment. ed. Jonathan Wren. *Bioinformatics* 2017;33(22):3679–81.
- Du Yanbin, Zhou Nan, Zha Wenting, Lv Yuan. Hypertension Is a Clinically Important Risk Factor for Critical Illness and Mortality in COVID-19: a Meta-Analysis. *Nutrition, metabolism, and cardiovascular diseases: NMCD* 2021;31(3):745–55.
- Ellinger Bernhard, et al. A SARS-CoV-2 Cytotoxicity Dataset Generated by High-Content Screening of a Large Drug Repurposing Collection. *Sci Data* 2021;8(1):70.
- Fricker Michael, et al. Neuronal Cell Death. *Physiol. Rev.* 2018;98(2):813–80.
- Gao Yue, et al. Machine Learning Based Early Warning System Enables Accurate Mortality Risk Prediction for COVID-19'. *Nat Commun* 2020;11(1):5033 <https://www.nature.com/articles/s41467-020-18684-2> November 13, 2020.
- Gaze David C. Clinical Utility of Cardiac Troponin Measurement in COVID-19 Infection. *Ann. Clin. Biochem.* 2020;57(3):202–5.
- Hansen David V, Hanson Jesse E, Sheng Morgan. Microglia in Alzheimer's Disease. *J. Cell Biol.* 2018;217(2):459–72.
- Harrell FE, et al. Evaluating the Yield of Medical Tests. *JAMA* 1982;247(18):2543–6.
- He Xingrui, et al. Selective Tyk2 Inhibitors as Potential Therapeutic Agents: a Patent Review (2015–2018). *Expert Opin Ther Pat* 2019;29(2):137–49.
- Heagerty Patrick J, Zheng Yingye. 'Survival Model Predictive Accuracy and ROC Curves'. *Biometrics* 2005;61(1):92–105.
- Himmelsbach Kiyoshi, Hildt Eberhard. The Kinase Inhibitor Sofarfenib Impairs the Antiviral Effect of Interferon  $\alpha$  on Hepatitis C Virus Replication. *Eur. J. Cell Biol.* 2013;92(1):12–20. <https://www.sciencedirect.com/science/article/pii/S0171933512001574> November 21, 2021.
- Inde Zintis, et al. Age-Dependent Regulation of SARS-CoV-2 Cell Entry Genes and Cell Death Programs Correlates with COVID-19 Severity. *Sci Adv* 2021;7(34):eab8609.
- Ip, Nancy Yuk-yu et al., 2015. 'STAT3 and TYK2 as Drug Targets for Neurodegenerative Diseases'. <https://patents.google.com/patent/CN102112879B/en> (September 20, 2021).
- Ishwaran Hemant, Kogalur Udaya B, Blackstone Eugene H, Lauer Michael S. Random Survival Forests. *Ann Appl Stat* 2008;2(3):841–60.
- Jakob Carolin EM, et al. Design and Evaluation of a Data Anonymization Pipeline to Promote Open Science on COVID-19'. *Sci Data* 2020;7(1):435.
- Jakob Carolin EM, et al. Prediction of COVID-19 Deterioration in High-Risk Patients at Diagnosis: an Early Warning Score for Advanced COVID-19 Developed by Machine Learning. *Infection* 2021. <https://link.springer.com/10.1007/s15010-021-01656-z> October 29, 2021.
- Jones Aaron, et al. External Validation of the 4C Mortality Score among COVID-19 Patients Admitted to Hospital in Ontario, Canada: a Retrospective Study. *Sci Rep* 2021;11(1):18638. <https://www.nature.com/articles/s41598-021-97332-1> October 21, 2021.
- Kaplan EL, Meier Paul. Nonparametric Estimation from Incomplete Observations. *J Am Stat Assoc* 1958;53(282):457–81. <https://www.tandfonline.com/doi/abs/10.1080/01621459.1958.10501452> November 22, 2021.
- Kar Sujay, et al. Multivariable Mortality Risk Prediction Using Machine Learning for COVID-19 Patients at Admission (AICOVID). *Sci Rep* 2021;11(1):12801. <https://www.nature.com/articles/s41598-021-92146-7> October 18, 2021.
- Katzman Jared, et al. DeepSurv: personalized Treatment Recommender System Using a Cox Proportional Hazards Deep Neural Network. *BMC Med Res Methodol* 2018;18(1). <http://arxiv.org/abs/1606.00931> March 22, 2018.
- Khan, Md Hasinur Rahaman, and J. Ewart H. Shaw. 2013. 'Variable Selection for Survival Data with A Class of Adaptive Elastic Net Techniques'. *arXiv:1312.2079 [stat]*. <http://arxiv.org/abs/1312.2079> (October 18, 2021).
- Krasemann Susanne, et al. The blood-brain barrier is dysregulated in COVID-19 and serves as a cns entry route for SARS-CoV-2, Rochester, NY: Social Science Research Network; 2021. SSRN Scholarly Paper <https://papers.ssrn.com/abstract=3828200> October 21, 2021.
- Li Guangdi, De Clercq Erik. Therapeutic Options for the 2019 Novel Coronavirus (2019-nCoV). *Nature Reviews Drug Discovery* 2020;19(3):149–50. <https://www.nature.com/articles/d41573-020-00016-0> November 21, 2021.
- Lundberg, Scott, and Su-In Lee. 2017. 'A Unified Approach to Interpreting Model Predictions'. *arXiv:1705.07874 [cs, stat]*. <http://arxiv.org/abs/1705.07874>.
- Mahdavi Mahdi, et al. A Machine Learning Based Exploration of COVID-19 Mortality Risk. *PLoS ONE* 2021;16(7):e0252384. <https://journals.plos.org/plosone/article?id=10.1371/journal.pone.0252384> October 18, 2021.
- Mathieu Edouard, et al. A Global Database of COVID-19 Vaccinations'. *Nature Human Behaviour* 2021;5(7):947–53. <https://www.nature.com/articles/s41562-021-01122-8> October 18, 2021.
- Meinhardt Jenny, et al. Olfactory Transmucosal SARS-CoV-2 Invasion as a Port of Central Nervous System Entry in Individuals with COVID-19'. *Nat. Neurosci.* 2021;24(2):168–75. <https://www.nature.com/articles/s41593-020-00758-5> October 18, 2021.
- O'Driscoll Megan, et al. Age-Specific Mortality and Immunity Patterns of SARS-CoV-2'. *Nature* 2021;590(7844):140–5.
- Paek Jin Hyuk, et al. Severe Acute Kidney Injury in COVID-19 Patients Is Associated with in-Hospital Mortality. *PLoS ONE* 2020;15(12):e0243528.
- Pan Pan, et al. SARS-CoV-2 N Protein Promotes NLRP3 Inflammation Activation to Induce Hyperinflammation'. *Nat Commun* 2021;12(1):4664.
- Porro Chiara, Ciacciulli Antonia, Panaro Maria Antonietta. The Regulatory Role of IL-10 in Neurodegenerative Diseases. *Biomolecules* 2020;10(7):1017.
- Qeadan Fares, et al. Prognostic Values of Serum Ferritin and D-Dimer Trajectory in Patients with COVID-19'. *Viruses* 2021;13(3):419.
- Qin Hongwei, et al. Inhibition of the JAK/STAT Pathway Protects Against  $\alpha$ -Synuclein-Induced Neuroinflammation and Dopaminergic Neurodegeneration.

- The Journal of Neuroscience: The Official Journal of the Society for Neuroscience 2016;36(18):5144–59.
- [48] Ryan Logan, et al. Mortality Prediction Model for the Triage of COVID-19, Pneumonia, and Mechanically Ventilated ICU Patients: a Retrospective Study. *Annals of Medicine and Surgery* 2020;59:207–16. <http://www.sciencedirect.com/science/article/pii/S2049080120303496> December 8, 2020.
- [49] Sattar Abdus, Sinha Sanjoy K, Morris Nathan J. A Parametric Survival Model When a Covariate Is Subject to Left-Censoring. *J Biom Biostat* 2012;3(2). Suppl <https://www.ncbi.nlm.nih.gov/pmc/articles/PMC3852406/> November 21, 2021. doi:10.4172/2155-6180.S3-002.
- [50] Scherbaum Raphael, et al. Clinical Profiles and Mortality of COVID-19 Inpatients with Parkinson's Disease in Germany. *Movement Disorders* 2021;36(5):1049–57. <https://onlinelibrary.wiley.com/doi/abs/10.1002/mds.28586> October 18, 2021.
- [51] Schmid Matthias, Potapov Sergej. A Comparison of Estimators to Evaluate the Discriminatory Power of Time-to-Event Models. *Stat Med* 2012;31(23):2588–609.
- [52] Schultz Bruce, et al. A Method for the Rational Selection of Drug Repurposing Candidates from Multimodal Knowledge Harmonization. *Sci Rep* 2021;11(1):11049.
- [53] Schwab Patrick, et al. Real-Time Prediction of COVID-19 Related Mortality Using Electronic Health Records'. *Nat Commun* 2021;12(1):1058. <https://www.nature.com/articles/s41467-020-20816-7> March 25, 2021.
- [54] Stringer Dominic, et al. The Role of C-Reactive Protein as a Prognostic Marker in COVID-19'. *Int J Epidemiol* 2021;50(2):420–9.
- [55] Stukalov Alexey, et al. Multilevel Proteomics Reveals Host Perturbations by SARS-CoV-2 and SARS-CoV'. *Nature* 2021:1–11.
- [56] Uno Hajime, et al. On the C-Statistics for Evaluating Overall Adequacy of Risk Prediction Procedures with Censored Survival Data. *Stat Med* 2011;30(10):1105–17.
- [57] Vaid Akhil, et al. Machine Learning to Predict Mortality and Critical Events in a Cohort of Patients With COVID-19 in New York City: model Development and Validation. *J. Med. Internet Res.* 2020;22(11):e24018. <https://www.jmir.org/2020/11/e24018/> November 13, 2020.
- [58] Vieira Davi, Gimenez Gabriel, Marmorela Guilherme, Estima Vitor. XGBoost Survival Embeddings: improving Statistical Properties of XGBoost Survival Analysis Implementation. *Loft. Python* 2021 August 9, 2021. <http://github.com/loft-br/xgboost-survival-embeddings>.
- [59] Vignatelli Luca, et al. Risk of Hospitalization and Death for COVID-19 in People with Parkinson's Disease or Parkinsonism. *Movement Disorders: Official Journal of the Movement Disorder Society* 2021;36(1):1–10.
- [60] Wan Jun, et al. 'Tyk2/STAT3 Signaling Mediates Beta-Amyloid-Induced Neuronal Cell Death: implications in Alzheimer's Disease. *The Journal of Neuroscience: The Official Journal of the Society for Neuroscience* 2010;30(20):6873–81.
- [61] Wang Shuo, Yuan Yu-He, Chen Nai-Hong, Wang Hong-Bo. The Mechanisms of NLRP3 Inflammasome/Pyroptosis Activation and Their Role in Parkinson's Disease. *Int. Immunopharmacol.* 2019;67:458–64.
- [62] Weibull. A Statistical Distribution Function of Wide Applicability. *J Appl Mech* 1951;18(3):293–7.
- [63] Weng Lin-Man, Su Xuan, Wang Xue-Qiang. Pain Symptoms in Patients with Coronavirus Disease (COVID-19): a Literature Review. *J Pain Res* 2021;14:147–59.
- [64] Werfel Stanislas, et al. Development and Validation of a Simplified Risk Score for the Prediction of Critical COVID-19 Illness in Newly Diagnosed Patients. *J. Med. Virol.* 2021;93(12):6703–13. <https://onlinelibrary.wiley.com/doi/abs/10.1002/jmv.27252> October 22, 2021.
- [65] Wool Geoffrey D, Miller Jonathan L. The Impact of COVID-19 Disease on Platelets and Coagulation. *Pathobiology* 2021;88(1):15–27.
- [66] Wu Yichao. Elastic Net for Cox's Proportional Hazards Model with a Solution Path Algorithm. *Stat Sin* 2012;22(1). <http://www3.stat.sinica.edu.tw/statistica/J22N1/J22N112/J22N112.html> October 18, 2021.
- [67] Zaliani Andrea, Vangeel Laura, Reinshagen Jeanette, Iaconis Daniela. Cytopathic SARS-Cov2 screening on VERO-E6 cells in a large repurposing effort. *EMBL-EBI*; 2020. September 20, 2021. [https://www.ebi.ac.uk/chembl/document\\_report\\_card/CHEMBL4495565](https://www.ebi.ac.uk/chembl/document_report_card/CHEMBL4495565).
- [68] Zhang Zhongheng. Parametric Regression Model for Survival Data: weibull Regression Model as an Example. *Ann Transl Med* 2016;4(24):484. <https://www.ncbi.nlm.nih.gov/pmc/articles/PMC5233524/> October 21, 2021.
- [69] Zheng Yi, et al. Severe Acute Respiratory Syndrome Coronavirus 2 (SARS-CoV-2) Membrane (M) Protein Inhibits Type I and III Interferon Production by Targeting RIG-I/MDA-5 Signaling. *Signal Transduction and Targeted Therapy* 2020;5(1):299.
- [70] Zhou Yadi, et al. Network Medicine Links SARS-CoV-2/COVID-19 Infection to Brain Microvascular Injury and Neuroinflammation in Dementia-like Cognitive Impairment. *Alzheimer's Research & Therapy* 2021;13(1):110 October 18, 2021. doi:10.1186/s13195-021-00850-3.
- [71] Zou Hui, Hastie Trevor. Regularization and Variable Selection via the Elastic Net. *Journal of the Royal Statistical Society: Series B (Statistical Methodology)* 2005;67(2):301–20.